Quantitative proteomic study reveals differential expression of matricellular proteins between fibrous dysplasia and cemento-ossifying fibroma pathogenesis

Duarte-Andrade, Filipe Fideles; Pereira, Thais dos Santos Fontes; Vitório, Jéssica Gardone; Diniz, Marina Gonçalves; Amorim, Larissa Stefhanne Damasceno; Nawrocki, Arkadiusz; Felicori, Liza Figueiredo; De Marco, Luiz; Gomes, Carolina Cavaliéri; Larsen, Martin R.; Melo-Braga, Marcella Nunes; Gomez, Ricardo Santiago

Published in:
Journal of Oral Pathology and Medicine

DOI:
10.1111/jop.13282

Publication date:
2022

Document version:
Accepted manuscript

Citation for pulished version (APA):
Duarte-Andrade, F. F., Pereira, T. D. S. F., Vitório, J. G., Diniz, M. G., Amorim, L. S. D., Nawrocki, A., Felicori, L. F., De Marco, L., Gomes, C. C., Larsen, M. R., Melo-Braga, M. N., & Gomez, R. S. (2022). Quantitative proteomic study reveals differential expression of matricellular proteins between fibrous dysplasia and cemento-ossifying fibroma pathogenesis. *Journal of Oral Pathology and Medicine*, *51*(4), 405-412. https://doi.org/10.1111/jop.13282

PROFESSOR RICARDO SANTIAGO GOMEZ (Orcid ID : 0000-0001-8770-8009)

DR THAÍS DOS SANTOS FONTES PEREIRA (Orcid ID : 0000-0002-1632-1533)

Article type : Original Article

Quantitative proteomic study reveals differential expression of matricellular proteins between fibrous dysplasia and cemento-ossifying fibroma pathogenesis

Filipe Fideles **Duarte-Andrade**[1,#]; Thais dos Santos Fontes **Pereira**[1,#]; Jéssica Gardone **Vitório**[1,#]; Marina Gonçalves **Diniz**[2]; Larissa Stefhanne Damasceno **Amorim**[1]; Arkadiusz **Nawrocki**[2]; Liza Figueiredo **Felicori**[4]; Luiz De **Marco**[3]; Carolina Cavaliéri **Gomes**[2]; Martin R. **Larsen**[2]; Marcella Nunes **Melo-Braga**[4,*]; Ricardo Santiago **Gomez**[1,*]

# These authors contributed equally to this study

[1] Department of Oral Surgery and Pathology, School of Dentistry, Universidade Federal de Minas Gerais (UFMG), Belo Horizonte, Brazil

[2] Department of Pathology, Biological Sciences Institute, Universidade Federal de Minas Gerais (UFMG), Belo Horizonte, Brazil

[3] Department of Surgery, School of Medicine, Universidade Federal de Minas Gerais.(UFMG), Belo Horizonte, Brazil

[4] Department of Biochemistry and Immunology, Biological Sciences Institute, Universidade Federal de Minas Gerais (UFMG), Belo Horizonte, Brazil

[5] Department of Biochemistry and Molecular Biology, University of Southern Denmark (SDU), Odense, Denmark

*Correspondence to:

Ricardo Santiago Gomez, Department of Oral Surgery and Pathology, School of Dentistry, UFMG, Av. Presidente Antônio Carlos, 6627, 31270-901, Belo Horizonte, Minas Gerais, Brazil. E-mail: rsgomez@ufmg.br

Marcella Nunes Melo-Braga, Department of Biochemistry and Immunology, Biological Sciences Institute, UFMG, Av. Presidente Antônio Carlos, 6627, 31270-901, Belo Horizonte, Minas Gerais, Brazi. E-mail: marcellanm@ufmg.br / marcelanmb@gmail.com

ACKNOWLEDGEMENTS

This study was financed in part by the Coordination for the Improvement of Higher Education Personnel (CAPES)/Brazil, Finance code 001, National Council for Scientific and Technological Development (CNPq) and The Minas Gerais Research Funding Foundation (FAPEMIG). FFD-A, MNM-B and TSFP received CAPES scholarship and JGV received CNPq scholarship. CCG and RSG are research fellows at CNPq.

The VILLUM Center for Bioanalytical Sciences at the University of Southern Denmark is acknowledged for access to state-of-the-art Mass spectrometric instrumentation.

Thanks to all members from Protein Research Group at University of Southern Denmark, in special Andrea Maria Lorentzen, Vladimir Gorshkov and Vibeke Jørgensen for column and instruments support.

ABSTRACT

Background Fibrous dysplasia (FD) and cemento-ossifying fibroma (COF) are the most common gnathic fibro-osseous lesions. These diseases exhibit remarkable overlap of several clinicopathological aspects and differential diagnosis depends on the combination of histopathological, radiographic and clinical aspects. Their molecular landscape remain poorly characterized and herein we assessed their proteomic and phosphoproteomic profiles.

Methods The quantitative differences in protein profile of FD and COF were assessed by proteomic and phosphoproteomic analyses of formalin-fixed paraffin-embedded tissue samples. Pathway enrichment analyses with differentialy regulated proteins were performed.

Results FD and COF exhibited differential regulation of pathways related to extracellular matrix organization, cell adhesion, and platelet and erythrocytes activities. Additionally, these lesions demonstrated distinct abundance of proteins involved in osteoblastic differentiation and tumorigenesis and differential abundance of phosphorylation of Ser61 of Yes-associated protein 1 (YAP1).

Conclusions In summary, despite the morphological similarity between these diseases, our results demonstrated that COF and DF present numerous quantitative differences in their proteomic profiles.These findings suggest that these fibro-osseous lesions trigger distinct molecular mechanisms during their pathogenesis. Moreover, some proteins identified in our analysis could serve as potential biomarkers for differential diagnosis of these diseases after further validation.

Keywords: Proteomics; ossifying fibroma; fibrous dysplasia; bone tumors; fibro-osseous lesions

1 INTRODUCTION

Fibrous dysplasia (FD) and cemento-ossifying fibroma (COF) are the most common of the rare benign fibro-osseous lesions (BFOLs) of the craniofacial skeleton[1]. COF is a bone neoplasm that typically affects patients aged between 30 to 40 years, while FD is a developmental disease that occurs mainly from childhood to early adulthood and has a predilection for craniofacial bones and femur, although it can affect other skeletal bones[1–3]. The differential diagnosis of these lesions poses a challenge for pathologists and clinicians due to similarities in many clinical parameters[1,2]. Because these BFOLs exhibit different clinical evolution and require distinct therapeutic approaches, an accurate diagnosis is of core importance[2].

Although activating mutations of *GNAS1* represent a specific molecular signature of FD, these alterations cannot be identified in all cases of this disease[2]. In contrast, the molecular landscape of COF remains poorly characterized[4]. Thus, further studies are still needed to identify novel biomarkers with greater discriminatory power and to clarify the differences in the pathogenesis of these BFOLs[5].

Proteomics and phosphoproteomics are comprehensive approaches focused on the qualitative and quantitative analysis of total proteins and phosphorylated proteins, respectively[6,7]. Protein levels and protein phosphorylation regulates numerous biological events, for instance, signaling pathways that control cellular processes such as cell growth, division, metabolic events, apoptosis, and others[6,7,8].

In this study, we quantitatively compared the total proteome and phosphoproteome of BFOLs to clarify whether the differences in clinical aspects and etiologies are associated with differential expression of proteins and/or regulation of signaling networks.

2 METHODS

2.1 Samples and Subjects

Six convenience formalin-fixed paraffin-embedded (FFPE) tissue samples were obtained from the files of the Oral Pathology Service at UFMG, comprising confirmed cases of COF (n = 3) and FD (n = 3). The clinical data of these patients are presented in **Table 1**, and their diagnoses were reviewed by oral pathologists based on WHO recommendations[3]. This study was approved by the Institutional Ethics Committee (CAAE: 43925221.9.0000.5149).

2.2 Quantitative proteomic and phosphoproteomic analyses

2.2.1 Sample preparation

Protein extraction was performed according to minor adaptations on the protocol described by Piehowski et al., 2018[9]. Proteins were extracted from deparaffinized tissues using 1:1 of TFE:Tris (600 mM) and 50 mM ammonium bicarbonate (AMBIC) containing a phosphatases and proteases inhibitors

cocktail. Samples were incubated at 95°C for 90 min and they were centrifuged at 14000 *g* for 5 minutes at 4°C. Supernatants were reduced with 5 mM dithiothreitol for 1 h at 37°C and alkylated with 40 mM iodoacetamide for 30 min at room temperature at dark. Subsequently, samples were diluted fivefold with 50 mM AMBIC buffer and digested overnight at 37°C with trypsin (1:50 - enzyme: substrate ratio). Peptides were desalted using Sep-Pak C18 solid-phase extraction cartridges (Waters Corporation, Massachusetts, USA) according to manufacturer's instructions. Peptides were quantified using the Qubit Protein Assay Kit (ThermoFisher, NY, USA) in a Qubit fluorometer (ThermoFisher, NY, USA) and twenty-five microgram of each sample was completely dried using a SpeedVac for the labeling.

Samples were labeled with TMT10plex™ isobaric tags (**Table 1, Fig 1**) (ThermoFisher, NY, USA). Peptides were initially reconstituted with 34 µL of 100 mM triethylammonium bicarbonate (TEAB) and mixed with 0.2 mg isobaric TMT dissolved in 10 µL of acetonitrile (**Table 1**, **Fig 1**). After incubation for 1 h at room temperature, the efficiency of labeling was checked by MALDI analysis. Subsequently, the reaction was quenched at room temperature with 8 µL of 5% hydroxylamine in 100 mM TEAB for 15 min. Samples were combined in a single tube and dried in a SpeedVac concentrator**.** Finally, phosphopeptide enrichment was performed with titanium dioxide (TiO_2) chromatography according to a previously published protocol[7]. The unbound fraction was also collected for the analysis of the total proteome (**Fig 1**).

2.2.2 High pH Reversed-Phase Fractionation

The peptides for analysis of the total proteome were resuspended in 20 mM ammonium formate pH 9.3 (solution A) and fractionated by HPLC (Ultimate 3000 HPLC) (Dionex, Sunnyvale, CA, USA), using a C18 Acquity UPLC M-Class CSH 1.7 µm, 300 µm X 100 mm column (Waters) in a flow of 10 µL/min. Peptides were eluted by the following gradient expressed as a percentage of solvent B (20% solution A / 80% ACN): 2-40% for 27 min; 40-50% in 4 min; 50-70% in 4 min and 70-95% in 5 min. The eluting peptides were separated into 15 fractions, automatically concatenated into 5 final fractions plus the flow-through (FT) fraction, and collected in 96-well plates (**Fig 1**). The sample were dried by vacuum centrifugation before LC-MS/MS.

2.2.3 Data acquisition: liquid chromatography-tandem mass spectrometry (LC-MS/MS)

The phosphorylated peptides and the six fractions from the total proteome were resuspended in 0.1% formic acid and injected on the nanoflow HPLC EASYnLC (Thermo Scientific). The system consisted of two in-house made fused silica C18 capillary columns, a pre-column (2 cm and 100 nm inner diameter, 5 µm) and an analytical column (17 cm, 75 nm inner diameter, 3 µm). Solvent A was composed of 0.1% formic acid and solvent B was formed by 90% acetonitrile with 0.1% formic acid. The peptides from total proteome fractions were separated with the following chromatographic gradient (in percentage of solvent B): 1-7% for 3 min; 7-28% in 50 min; 28-45% in 10 min; 45-100% in 3 min, with the flow at 250 nL/min. The gradient used to separate the phosphorylated peptides was: 1-3% for 3 min; 3-22% in 120 min; 22-40% in 20 min; 40-95% in 3 min.

The eluting peptides from the analytical column were ionized by nanoelectrospray and analyzed by a Q-Exactive HF Orbitrap mass spectrometer (Thermo Fisher) working in data-dependent acquisition (DDA) mode. In the MS, the peptide ions of the total proteome and phosphoproteome were resolved in the orbitrap, with mass ranges between 400 to 1600 m/z and 350 to 1400 m/z, respectively, at 120,000 FWHM resolution. At each MS, the 15 most intense ions (Top 15) for the total proteome and the Top 10 for the phosphoproteome were selected for HCD fragmentation with a normalized collision energy of 34. The originated fragments were resolved in the orbitrap, mass range between 110 and 2000 m/z, and a resolution of 60,000 FWHM (total proteome) and 45,000 FWHM (phosphoproteome).

2.2.4 Data analysis

Raw data files were processed using Proteome Discoverer version 2.4.0.305 using the Sequest HT as the search engine for peptide identification against the Human Swiss-Prot database (20,366 entries, downloaded in 04-19-2020). The following parameters were used in the searches: trypsin was specified as cleavage enzyme, accepting a maximum of two missed cleavages;

carbamidomethylation of cysteine was set as a static modification, and oxidation of methionine, N-terminal protein acetylation, TMT modifications in lysine and peptide N-terminus were set as a dynamic modification. In the phosphoproteome analysis, phosphorylation of serine, threonine, and tyrosine (STY) residues were also considered as variable modifications. The precursor mass tolerance and fragment mass tolerance were set to 10 ppm and 0.02 Da, respectively.

Quantification of the proteins and phosphopeptides was performed by the intensity of TMT reporter ions in their respective peptides. For each protein, the relative expression value was obtained by combining the intensities of their unique plus razor peptides. Potential contaminants were removed from the dataset before further analysis.

2.2.5 Statistical Analyses

Before statistical analyses, proteins and phosphorylated peptides intensities were $\log_2$ transformed and normalized by subtracting the median intensity in each condition, using Perseus v1.6.14.0. The phosphorylated peptides were also normalized by their respective proteins from the total proteome whenever possible[8]. LIMMA test was performed in NormalyzerDE to identify differential proteins, using p-value <0.05 combined with $\log_2$ fold change cutoff of ≥ 0.58 or ≤-0.58 as the threshold of significance. Multivariate analyses were conducted on Metaboanalyst version 4.0.

2.4 Gene Ontology (GO) and Pathway Enrichment Analyses

Ontology analyses were performed on PantherDB and EnrichR. Pathway enrichment analysis was conducted in PathDIP 4. Protein-protein interaction network was build in STRING Version 11.0.

3 RESULTS

3.1. Overview and quality control of total proteome and phosphoproteome data

In general, 570 proteins were confidently identified in the total proteome (**Supplementary table 1**), while 58 phosphopeptides, corresponding to 69 phosphosites in 40 proteins were quantified with a 95% probability of correct phosphorylation site localization (**Supplementary table 2**).

To assess the quality of the extraction, an ontology enrichment analysis was performed based on the Jensen TISSUE database. Bone was found as the most significant tissue (**Supplementary Figure 1A**). Accordingly, classic bone proteins, such as osteopontin, were observed in our dataset, which is in accordance with the fibrous-osseous origin of these diseases. Furthermore, GO analysis of cellular components revealed that the proteins were distributed both in intracellular and extracellular compartments **(Supplementary Figure 1B)**, indicating that the extraction procedures were adequately comprehensive.

3.2 COF and FD exhibit differential regulation of proteins and biological pathways

In order to evaluate whether COF and FD exhibit an overall distinct proteomic profile, an hierarchical cluster analysis was performed. The lesions tended to group in different clusters, except for one COF sample that grouped with the FD samples **(Fig 2A)**.

The levels of 51 proteins were found to be significantly altered between COF and FD (**Fig 2B, Supplementary Table 1**). Interestingly, the abundance of several significantly regulated proteins exhibited intragroup variation among COF samples (**Fig 2B**). Explanations for this observation could be related to the inherent phenotypic variability of fibro-osseous lesions, for instance, the type of mineralized components and their proportion[10] or possible differences in the molecular landscape of the lesions[5].

A pathway enrichment analysis was performed with the up-regulated genes in the FD samples (**Table 2** and **Supplementary Table 3**). Pathways related to platelet and erythrocytes activities, association of TriC/CCT with target proteins during biosynthesis, and extracellular matrix (ECM) organization were observed amongst the 10 most significantly enriched biological pathways

in FD (**Table 2**). Similarly, a pathway analysis was performed with proteins with increased abundance in COF, but no significant results were retrieved (data not shown).

In a more detailed analysis of pathway enrichment results, it was noted that numerous biological pathways related to the extracellular matrix (ECM) and associated processes were enriched (**Fig 3A**). Consistently, 12 of the 51 significantly altered proteins (either up- or downregulated) were either "core" ECM or ECM-associated proteins (**Fig 3B**). Moreover, according to experimental and prediction data, most of these proteins interacted with each other (**Fig 3C**).

3.3 Quantitative differences are observed in the phosphorylation profile of COF and FD

We evaluated by quantitative phosphoproteomic analysis whether different signaling pathways are triggered during COF and FD pathogenesis. Statistical analysis of the phosphoproteome data revealed that the phosphorylation of Ser61 of the transcriptional coactivator YAP1 was significantly increased in COF (**Supplementary Table 2**). Although not statistically significant, the levels of phosphorylation of Ser304 and Ser307 of RPLP0, Ser58 and Ser61 of NUCKS1, and T150 of MARCKS were consistently altered between both diseases (**Supplementary Table 2**).

4 DISCUSSION

Comparative studies of fibro-osseous lesions investigating the abundance of proteins are scarce and have been mostly focused on assessing non-collagenous markers of osteogenesis and bone resorption by immunohistochemistry[10–12]. Thus, in order to further elucidate the differences in the pathogenesis of these lesions, we performed a quantitative evaluation of their phosphoproteome and total proteome.

Our results showed that several proteins involved in ECM organization and other associated processes are differentially expressed between FD and COF (**Fig 4**). Among these proteins, biglycan (BGN) and thrombospondin 1 (THBS1) are involved in the regulation of the availability and activation of a

modulator of osteoblastic fate, the transforming growth factor-β (TGF-β)[13], respectively. THBS1 has also been implicated in the modulation of multiple aspects of tumor progression, including cell adhesion, proliferation, apoptosis, angiogenesis, and others[14]. In addition, tenascin C (TNC) abundance was also increased in FD and this glycoprotein is associated with osteogenic differentiation[15], which support that these lesions have differences in the degree of differentiation and that the distinct regulation of matricellular proteins contributes to this variation. Further supporting this hypothesis, the levels of alpha-2-macroglobulin (α_2m), which influences the availability of osteogenic growth peptide (OGP) and modulates TGF-β1 and TGF-β2 activities[16,17], were decreased in COF. Recently, it has been proposed that activating *GNAS1* mutations may influence the expression of ECM-related genes[18]. Therefore, the differential regulation of ECM proteins levels between these diseases may arise from the differences in their genetic background. Notably, alterations of ECM components in FD have been previously shown in studies evaluating the gene expression of affected subjects compared to unaffected controls[19,20].

Pigment epithelium-derived factor (PEDF) is a glycoprotein encoded by SERPINF1 gene that has multiple functions in bone biology[21]. In our current study, PEDF levels were consistently increased in all FD samples. PEDF has been implicated in the osteogenic differentiation of mesenchymal stem cells, exerting negative effects on adipogenesis via the activation of WNT/β-catenin signaling[21,22]. Considering the importance of WNT/β-catenin dysregulation in FD development[23], it is reasonable to speculate that the increased levels of PEDF might contribute to alterations in the activity of this signaling pathway in this lesion. Also suggesting a pivotal role of this protein in FD pathogenesis, a study assessing the gene expression in FD tissues in comparison to healthy controls demonstrated significant alteration in the levels of PEDF transcripts[20]. Furthermore, our group previously demonstrated that WNT/β-catenin pathway is potentially involved in COF pathogenesis[4]. Thus, these results may also indicate that FD and COF exhibit distinct factors governing the dysregulation of this biological pathway, but further investigation is needed to confirm this hypothesis.

In our study, pathway enrichment analysis revealed that several proteins involved in platelet and erythrocyte activities are increased in FD in comparison with COF. These findings are in agreement with a previous study based on histomorphometric analyses demonstrating that FD presents higher intralesional vascular content[24]. Although our findings support the occurrence of differences between these diseases, further investigation is necessary to rule out the possibility that the enrichment of blood-related pathways is not due to contamination with extralesional blood during surgical procedures. To our knowledge, other investigations solely assessed the presence or absence of microvessels and/or hemorrhagic foci without any quantitative parameters. Hence, further investigation is still necessary, including a quantitative analysis of intralesional microvessel density markers in these diseases.

Previous reports showed that the abundance of dentin matrix acidic phosphoprotein 1 (DMP1) and osteopontin were not significantly altered between these lesions by immunohistochemical evaluations[11]. Similarly, our proteomic approach demonstrated no significant alteration in their abundance, further corroborating that these proteins are not useful as differential biomarkers of FD and COF. In contrast, the levels of several proteins were consistently altered in our total proteome analysis and could serve as potential differential biomarkers, such as PEDF, α_2m, THBS1 and others, but further analyses are required.

In a previous immunohistochemical evaluation of the distribution of S100 proteins in FD and COF, it was noted that S100-A4 and S100-A6 are expressed in the fibrous stroma and the hard-tissue-forming cells of these lesions[25]. However, no statistical evaluation of the results was performed in this report[25]. In our study, the abundance of these proteins was significantly increased in COF in comparison to FD. Several reports have demonstrated that S100-A4 regulates the differentiation of osteoblastic progenitor cells into osteoblasts[26]. Increased expression of S100-A4 has been associated with reduced differentiation of osteoblasts, mineralization, and the expression of osteoblastic markers such as osteocalcin[26,27]. Similarly, S100-A6 overexpression has also been implicated in the inhibition of osteogenic differentiation, besides promoting cell proliferation[28]. Thus, it could be argued that these proteins could be involved in the disturbances of osteoblastic differentiation in COF.

Increased phosphorylation of Ser61 of Yes-associated protein 1 (YAP1) in COF was the only statistically significant alteration identified in our phosphoproteome analysis most likely due to the poor recovery of phosphorylated peptides from FFPE samples. Interestingly, YAP1 is a transcriptional activator that stimulates several biological process, including cell differentiation, survival, migration, and proliferation and constitutes a pivotal mediator of the Hippo Pathway[29]. The phosphorylation of Se61 inhibits YAP transcriptional activity and is predicted to inactivate the protein function[29]. Since YAP1 was identified solely in the phosphoproteome analysis, normalization by total protein levels was not possible. Thus, further verification of the regulation of this phosphorylation site is needed.

The limitations of the present study include the limited number of phosphosites identified and small number of samples. Consistently, lower numbers of detected phosphopeptides in FFPE specimens were demonstrated in previous studies in comparison to optimal cutting temperature compound (OCT) preserved samples[9] and fresh frozen tissues[30]. Additionally, to our knowledge, most FFPE-based phosphoproteomics protocols were proposed for soft tissues[9,30]. Additional optimizations are required for proper extraction of phosphoproteins from mineralized tissues and hard-tissue-forming lesions. Future investigations should consider employing greater cohort sizes, OCT-embedded or fresh frozen tissues, and other extraction methods, quantification approaches, and MS-based techniques.

Fibro-osseous lesions show extensive phenotypic variability, including differences in cellularity, stage of differentiation of the osteoblasts, the degree and types of calcifications, the presence of osteoclasts, and others. All these aspects are known to influence protein expression and quantification. In agreement, Veltrini et al. (2019)[10] recently demonstrated the impact of these factors in the immunohistochemical profile of the non-collagenous proteins of these lesions, precluding the use of these proteins as differential diagnosis biomarkers. Moreover, our analyses suggested that the proteomic landscape of COF is diverse, in agreement with recent reports showing that the genomic background of this tumor is complex[5]. Considering that phosphorylation is a dynamic post-translational modification that controls and responds to different

biological stimuli, a major impact of the variability of the phenotypic aspects of these fibro-osseous lesions was expected on their phosphoproteome profile.

5 CONCLUSIONS

Although the small sample size limits our conclusions, this investigation of the proteome and phosphoproteome of COF and FD revealed that these diseases exhibit differential regulation of proteins involved in several biological pathways, including those related to platelet and erythrocytes activities and extracellular matrix organization. Additionally, many proteins identified in our analysis could serve as potential biomarkers for differential diagnosis of these diseases, following validation in larger cohorts of samples. Further research is required to confirm our results, to optimize proteomic evaluation of mineralized FFPE tissues and to increase the knowledge of the molecular pathogenesis of FD and COF.

REFERENCES

1. Nelson BL, Phillips BJ. Benign Fibro-Osseous Lesions of the Head and Neck. Head Neck Pathol 2019;13(3):466-475.
2. Pereira T dos SF, Gomes CC, Brennan PA, Fonseca FP, Gomez RS. Fibrous dysplasia of the jaws: Integrating molecular pathogenesis with clinical, radiological, and histopathological features. J Oral Pathol Med 2019;48(1):3-9.
3. El-Naggar AK, Chan, John KC, Grandis JR, Takata T, Slootweg PJ. World Health Organization Classification of Head and Neck Tumours.; 2017.
4. Pereira T dos SF, Diniz MG, França JA, et al. The Wnt/β-catenin pathway is deregulated in cemento-ossifying fibromas. Oral Surg Oral Med Oral Pathol Oral Radiol 2017;125(2):172-178.
5. Ma M, Liu L, Shi R, et al. Copy number alteration profiling facilitates differential diagnosis between ossifying fibroma and fibrous dysplasia of the jaws. Int J Oral Sci 2021;13(1).
6. Maes E, Mertens I, Valkenborg D, et al. Proteomics in cancer research: Are we ready for clinical practice? Crit Rev Oncol Hematol 2015;96(3):437-48.
7. Melo-Braga MN, Ibáñez-Vea M, Larsen MR, Kulej K. Comprehensive

protocol to simultaneously study protein phosphorylation, acetylation, and N-linked sialylated glycosylation. Methods Mol Biol 2015;1295:275-292.

8. Wu R, Dephoure N, Haas W, et al. Correct Interpretation of Comprehensive Phosphorylation Dynamics Requires Normalization by Protein Expression Changes. Mol Cell Proteomics 2011: 10(8): M111.009654.
9. Piehowski PD, Petyuk VA, Sontag RL, et al. Residual tissue repositories as a resource for population - based cancer proteomic studies. Clin Proteomics 2018;15(26):1-12
10. Veltrini VC, Figueira JA, Santin GC, de Sousa SCOM, de Araújo NS. Can non-collagenous proteins be employed for the differential diagnosis among fibrous dysplasia, cemento-osseous dysplasia and cemento-ossifying fibroma? Pathol Res Pract 2019;215(7):152450.
11. Toyosawa S, Yuki M, Kishino M, et al. Ossifying fibroma vs fibrous dysplasia of the jaw: molecular and immunological characterization. Mod Pathol 2007;20(3):389-396.
12. Elias LSA, Costa RF, Carvalho MA, et al. Markers of bone remodeling in neoplastic and bone-related lesions. Oral Surgery, Oral Med Oral Pathol Oral Radiol Endodontology 2010;110(5):624-631.
13. Alford AI, Kozloff KM, Hankenson KD. Extracellular matrix networks in bone remodeling. Int J Biochem Cell Biol 2015;65:20-31.
14. Huang T, Sun L, Yuan X, Qiu H. Thrombospondin-1 is a multifaceted player in tumor progression. Oncotarget 2017;8(48):84546-84558.
15. Morgan JM, Wong A, Yellowley CE, Genetos DC. Regulation of tenascin expression in bone. J Cell Biochem 2011;112(11):3354-3363.
16. Danielpour D, Sporn MB. Differential inhibition of transforming growth factor beta 1 and beta 2 activity by alpha 2-macroglobulin. J Biol Chem 1990;265(12):6973-6977.
17. Gavish H, Bab I, Tartakovsky A, et al. Human α2-macroglobulin is an osteogenic growth peptide-binding protein. Biochemistry 1997;36(48):14883-14888.
18. Raimondo D, Remoli C, Astrologo L, et al. Changes in gene expression

in human skeletal stem cells transduced with constitutively active Gsα correlates with hallmark histopathological changes seen in fibrous dysplastic bone. PLoS One 2020;15(1):1-22.

19. Kiss J, Balla B, Kósa JP, et al. Gene expression patterns in the bone tissue of women with fibrous dysplasia. Am J Med Genet Part A 2010;152(9):2211-2220.
20. Zhou SH, Yang WJ, Liu SW, et al. Gene expression profiling of craniofacial fibrous dysplasia reveals ADAMTS2 overexpression as a potential marker. Int J Clin Exp Pathol 2014;7(12):8532-8541.
21. Baxter-Holland M, Dass CR. Pigment epithelium-derived factor: a key mediator in bone homeostasis and potential for bone regenerative therapy. J Pharm Pharmacol 2018;70(9):1127-1138.
22. Gattu AK, Swenson ES, Iwakiri Y, et al. Determination of mesenchymal stem cell fate by pigment epithelium-derived factor (PEDF) results in increased adiposity and reduced bone mineral content. FASEB J 2013;27(11):4384-4394.
23. Regard JB, Cherman N, Palmer D, et al. Wnt/β-catenin signaling is differentially regulated by Gα proteins and contributes to fibrous dysplasia. Proc Natl Acad Sci USA 2011;108(50):20101-20106.
24. Shmuly T, Allon DM, Vered M, Chaushu G, Shlomi B, Kaplan I. Can Differences in Vascularity Serve as a Diagnostic Aid in Fibro-Osseous Lesions of the Jaws? J Oral Maxillofac Surg 2017;75(6):1201-1208.
25. Muramatsu Y, Kamegai A, Shiba T, et al. Histochemical characteristics of calcium binding S100 proteins and bone morphogenetic proteins in chondro-osseous tumors. Oncol Rep 1997;4:49-53.
26. Duarte WR, Shibata T, Takenaga K, et al. S100A4: A Novel Negative Regulator of Mineralization and Osteoblast Differentiation. J Bone Miner Res 2003;18(3):493-501.
27. Kim H, Lee YD, Kim MK, et al. Extracellular S100A4 negatively regulates osteoblast function by activating the NF-κB pathway. BMB Rep 2017;50(2):97-102.
28. Li Y, Wagner ER, Yan Z, et al. The calcium-binding protein S100A6 accelerates human osteosarcoma growth by promoting cell proliferation and inhibiting osteogenic differentiation. Cell Physiol

Biochem 2015;37(6):2375-2392.
29. Szulzewsky F, Holland EC, Vasioukhin V. YAP1 and its fusion proteins in cancer initiation, progression and therapeutic resistance. Developmental Biology 2021;475: 205-221.
30. Zeneyedpour L, Stingl C, Dekker LJM, et al. Phosphorylation ratio determination in fresh-frozen and formalin-fixed paraffin-embedded tissue with targeted mass spectrometry. J Proteome Res 2020;19(10):4179-4190.

TABLES

TABLE 1. Clinical characteristics of study participants and TMT labelling scheme for samples

Diagnoses	Age	Gender	Location	TMT Label
FD	23	Male	Maxilla	127C
FD	10	Female	Maxilla	128N
FD	23	Female	Maxilla	128C
COF	29	Female	Mandible	129N
COF	58	Female	Mandible	129C
COF	16	Male	Mandible	130N

TABLE 2. Top ten potentially upregulated pathways in FD

Pathway Source	Pathway Name	p-value	# of proteins found in pathway	q-value (FDR: BH-method)	q-value (Bonferroni)
Reactome	Association of TriC/CCT with target proteins during biosynthesis	7.37E-07	3	3.85E-04	3.85E-04
Reactome	Response to elevated platelet cytosolic Ca2+	3.51E-06	5	6.11E-04	1.83E-03
Reactome	Platelet degranulation	2.88E-06	5	7.51E-04	1.50E-03
PID	Syndecan-4-mediated signaling events	2.96E-05	3	3.87E-03	1.55E-02
Reactome	Platelet activation, signaling and aggregation	9.59E-05	5	6.26E-03	5.01E-02
Reactome	Chaperonin-mediated protein folding	7.27E-05	3	6.33E-03	3.80E-02
Reactome	Protein folding	7.27E-05	3	6.33E-03	3.80E-02

Reactome	Cooperation of PDCL (PhLP1) and TRiC/CCT in G-protein beta folding	6.77E-05	3	7.07E-03	3.53E-02
Reactome	Erythrocytes take up oxygen and release carbon dioxide	1.26E-04	2	7.29E-03	6.56E-02
Reactome	Extracellular matrix organization	1.55E-04	5	8.11E-03	8.11E-02

A FDR (BH: method) < 0.05 was used as cutoff of pathway enrichment analysis. Abbreviations: PID: the Pathway Interaction Database; FDR: False discovery Rate; BH method: Benjamini Hochberg method

FIGURE LEGENDS

Figure 1. Schematic representation of the quantitative proteomic and phosphoproteomic pipeline employed in the present study. Proteins were extracted from formalin-fixed paraffin-embedded (FFPE) tissue samples of confirmed cases of COF and FD. Cleavage of the proteins was performed with trypsin. Each sample was labeled with a distinct TMT10plex™ tag. Labeled samples were pooled and the phosphopeptides were enriched using TiO_2 chromatography. Both eluting flow-through (FT) and eluting (EL) pepetides during TiO_2 enrichment were collected to allow the analyses of the total proteome and phosphoproteome of the lesions, respectively. Subsequently, the total proteome was pre-fractionated into six fractions using an offline HPLC. Finally, the proteomic and phosphoproteomic data were acquired using a LC/MS/MS system. This illustration was created using BioRender.

Fig 2. Intragroup variation observed in the total proteome analysis of COF and FD. A. Hierarchical clustering dendrogram built using all identified proteins in the total proteome analysis. The following parameters were applied in MetaboAnalyst 4.0 for the dendrogram construction: distance measure: Euclidean and clustering algorithm: complete. **B.** Hierarchical clustering heatmap made with the differentially regulated proteins between COF and FD. Protein abundance across the samples is indicated by the color scale on the top right, varying from green (decreased) to red (increased)**.** The dendrograms in the the top and left side of the heatmap were also constructed using Euclidean distance and complete linkage.

Figure 3. Changes in the abundance and composition of matricellular and ECM-associated proteins may represent an important mechanism in the pathogenesis of fibro-osseous lesions. A. Biological pathways related to ECM and associated processes are potentially upregulated in FD. **B.** Twelve ECM and ECM-associated proteins were significantly altered between FD and COF. The annotation of the category of each protein was conducted with

Matrisome Annotator according to the MatrisomeDB divisions (Naba et al., 2016). **C.** Interaction network established among the "core" ECM and ECM-associated proteins according to known and predicted interactions, and other information such as text-mining, co-expression and protein homology. Considering the lack of any direct interaction among Chondroadherin (CHAD) and Tenascin (TNC) and the other proteins, these molecules are not displayed in the graph. The abundance of each protein in FD is specified by a color scale, in which green indicates decreased levels and red denote increased abundance. ECM: extracellular matrix

Figure 4. Proposed model of the molecular mechanisms involved in the pathogenesis of FD based on the proteomic and phosphoproteomic results. The increased cell growth, cell differentiation disturbances and enhanced cell survival in FD might be associated to alterations in the levels of ECM core and/or related proteins, which are able to regulate several mechanosensing pathways by ECM-receptor interaction, which trigger the transcription of several genes by a complex series of molecular events. Further analyses are needed to confirm this proposition. Question marks denote processes with conflicting descriptions in the literature that require careful interpretation. This model was constructed combining statistically significant findings of the total proteome and phosphoproteome analysis, results of pathway analysis, and information available on the literature, KEGG and Reactome pathway databases.

SUPPLEMENTARY MATERIALS

Supplementary Table 1 - List of proteins quantified and identified with at least two unique peptides, protein FDR confidence ≤ 1% and a minimum of 2 valid values in each group. In COF vs FD_log2FoldChange, red denote up-regulated proteins and green down-regulated proteins

Supplementary Table 2 - List of phosphopeptides unambiguously quantified and with a 95% probability of correct phosphorylation site localization. In COF vs FD_log2FoldChange, red denote up-regulated phosphopeptide, differential proteins were based on p-value <0.05 in addition to a log2 fold change cutoff > 0.58 or <-0.58.

Supplementary Table 3. Summary of the significantly enriched pathways and the proteins found in each biological process.

Figure S1. Ontology analyses performed with total proteome data. A. Ontology enrichment analysis based on Jensen TISSUE database. Results were ranked according to p-value and bone tissue was the most significantly enriched. **B.** GO-cellular component analysis demonstrating adequate extraction of intracellular and extracellular proteins. For simplification purpose, the PANTHER GO-slim module was used in this evaluation. Synapse part (GO:0044456) and synapse (GO:0045202) accounted for 0.20% each and were not included in graph elaboration.

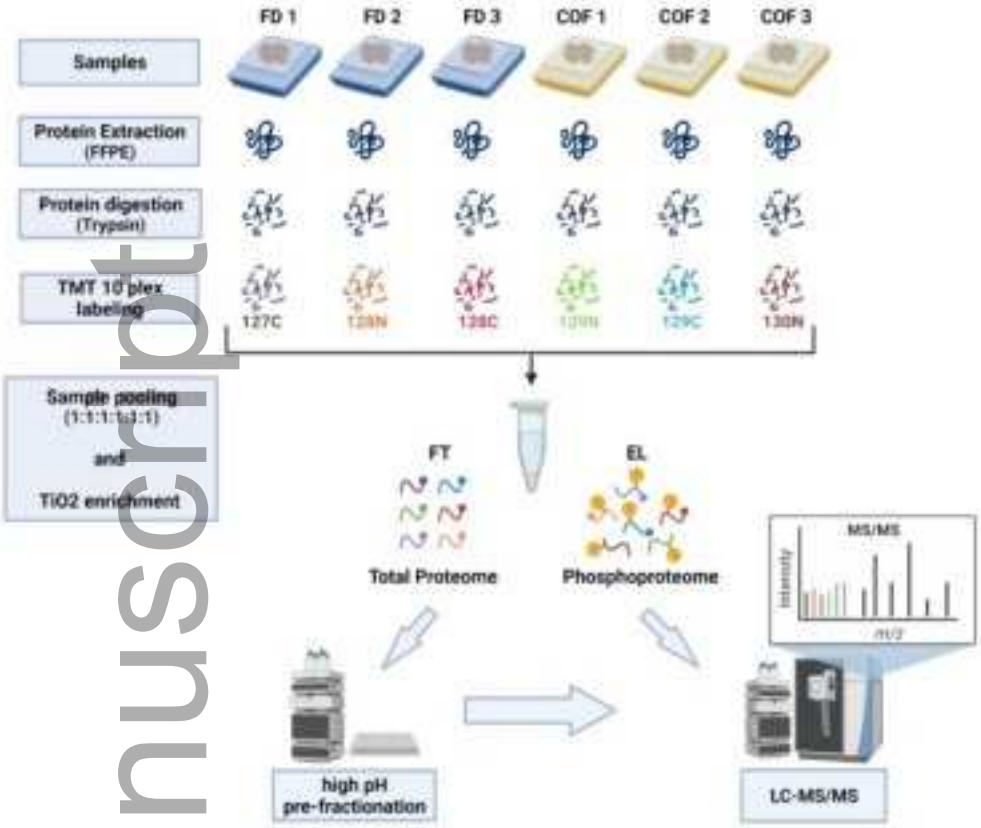

jop_13282_f1.jpeg

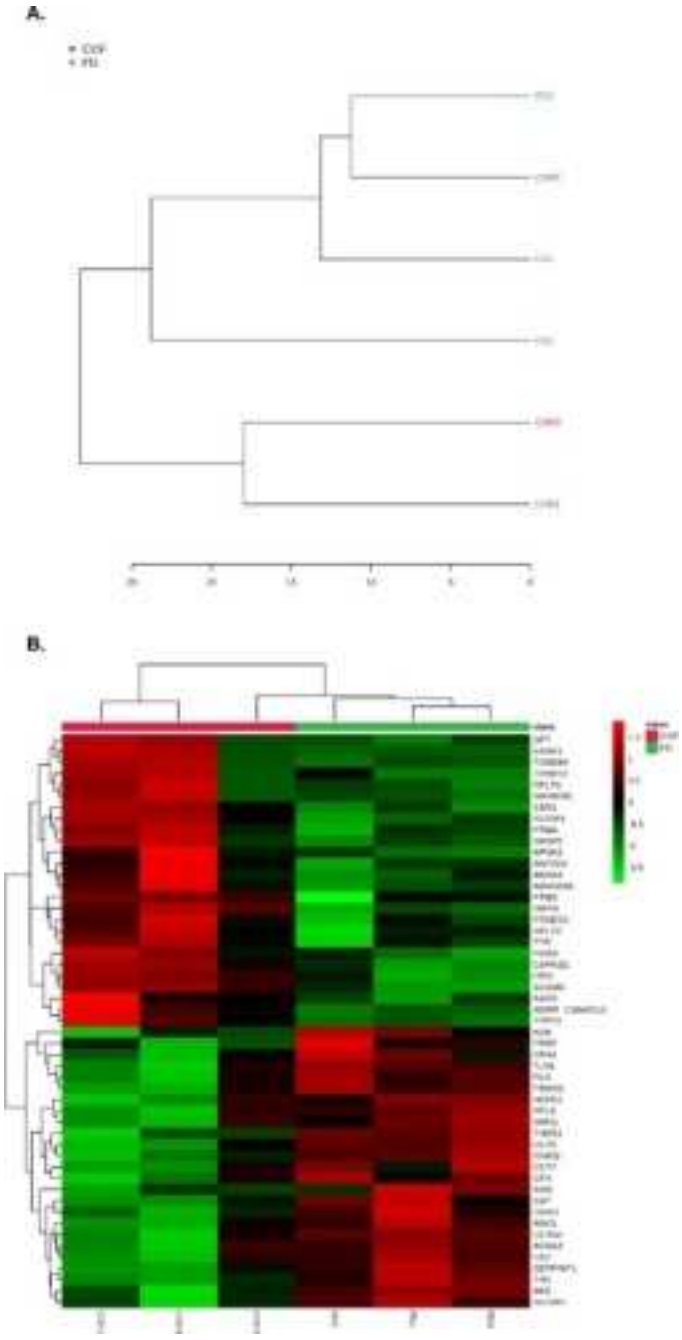

jop_13282_f2.png

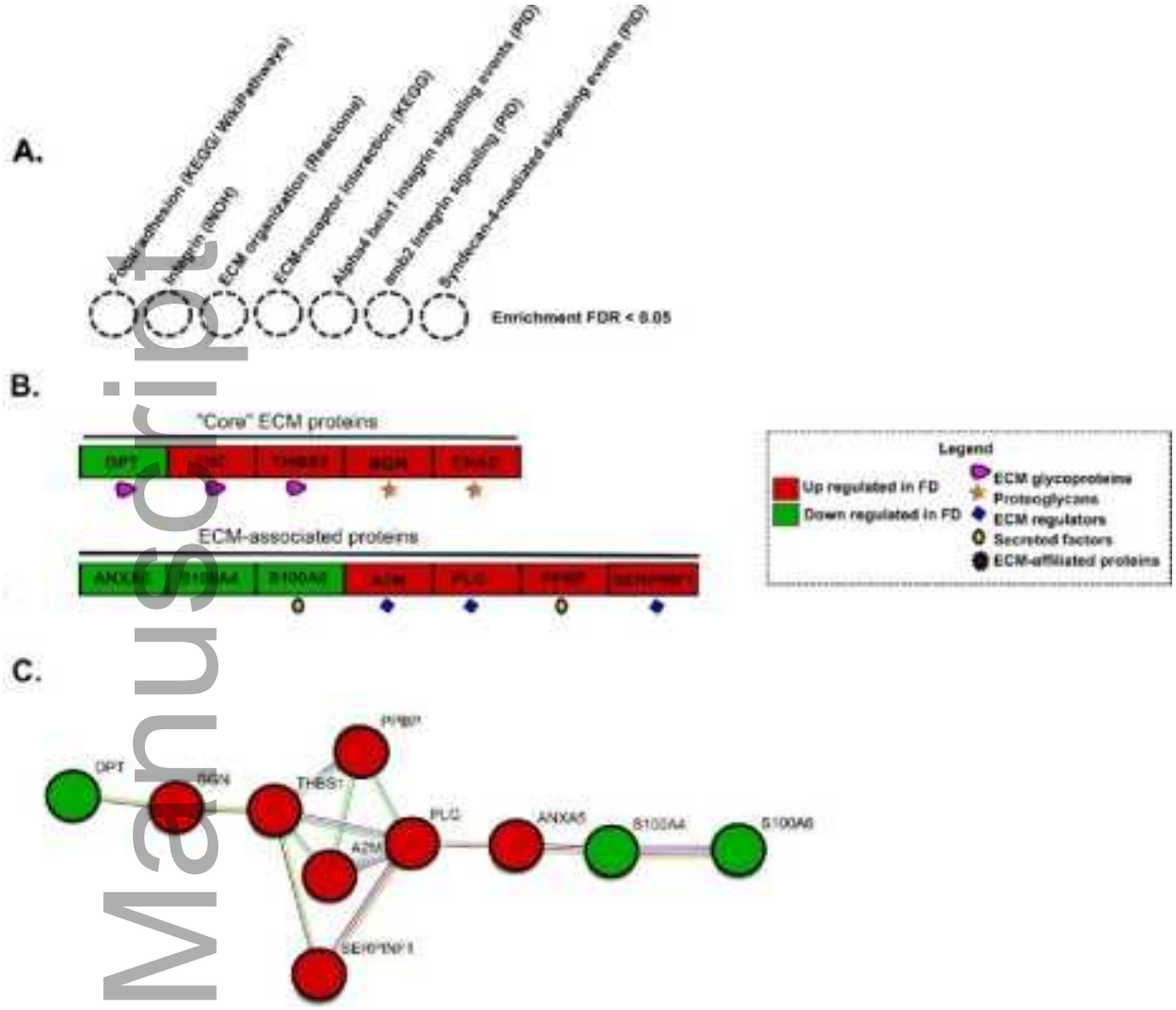

jop_13282_f3.png

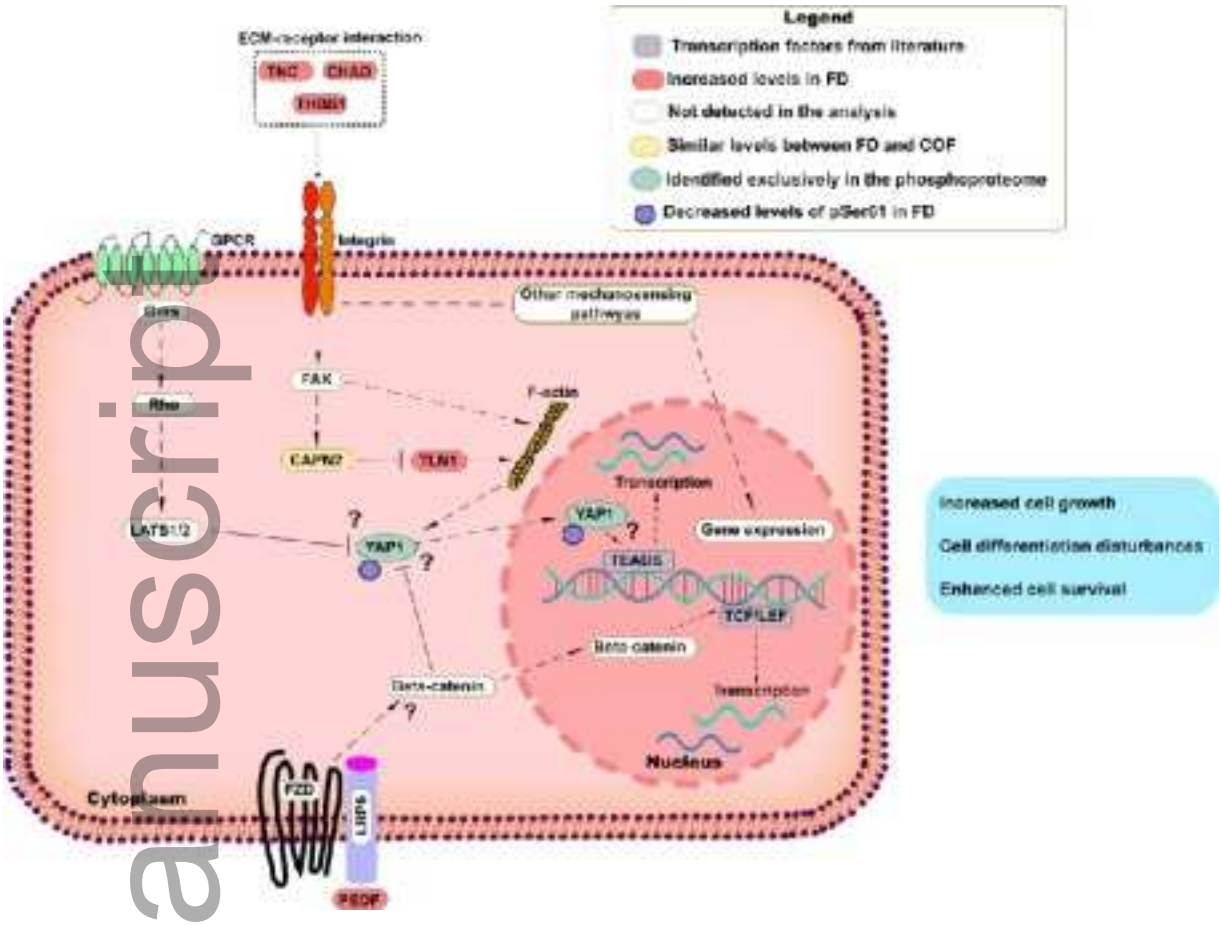

jop_13282_f4.png